Journal of Controlled Release 220 (2015) 245–252

Contents lists available at ScienceDirect

Journal of Controlled Release

journal homepage: www.elsevier.com/locate/jconrel

Comparative effect of gold nanorods and nanocages for prostate tumor hyperthermia

Ryan Robinson [a,b], Wiebke Gerlach [b,c], Hamidreza Ghandehari [a,b,c,*]

[a] Department of Bioengineering, University of Utah, Salt Lake City, UT 84112, USA
[b] Center for Nanomedicine, Nano Institute of Utah, Salt Lake City, UT 84112, USA
[c] Department of Pharmaceutics and Pharmaceutical Chemistry, University of Utah, Salt Lake City, UT 84112, USA

ARTICLE INFO

Article history:
Received 23 June 2015
Received in revised form 7 October 2015
Accepted 18 October 2015
Available online 23 October 2015

Keywords:
Gold nanocages
Gold nanorods
Photothermal therapy
Hyperthermia

ABSTRACT

Gold nanoparticles have been investigated as photothermal agents, drug delivery carriers, diagnostics, and theranostics. As long-term accumulation of nanoparticles in nontarget tissues is a growing concern, it is vital to establish biodistribution profiles, tumor uptake, and tissue residence times for each nano-based system. This study aimed to investigate the prostate tumor uptake, photothermal therapy mediated macromolecular delivery, acute and chronic biodistribution profiles, and organ residence time differences between two nanoparticles, i.e., gold nanocages and gold nanorods. These particles have tunable surface plasmon resonances in the near infrared, but dissimilar shapes. Gold nanocages and nanorods had very different light to heat transduction efficiencies, with gold nanocages requiring 18.4 times fewer particles and approximately half the gold mass of gold nanorods to achieve the same heating profile given a constant laser intensity. It was also observed that while the photothermal macromolecular delivery enhancements were similar for the two systems when dosed by optical density, the tumoral uptake and biodistribution profiles for each of these shapes differed, with the nanocages residing in the liver, kidneys and spleen for less time than the nanorods. Additionally, it was observed that the nanocages were excreted from the body at a higher percentage of injected dose than the nanorods at both the 7 and 28 day time points. These findings have implications for the use of these constructs in diagnostic and therapeutic applications.

1. Introduction

Advances in the synthesis and characterization of gold nanoparticles have led to an expanded control over shape, size, and surface chemistry. This has resulted in an array of work exploring the applications of plasmon-resonant nanoparticles in the treatment and diagnosis of malignancies [1–3] Prostate cancer is the second most common cancer, and the second leading cause of cancer related death in American men [4]. Localized prostate cancer accounts for 81% of these cases and the most common current methods of treatment are surgery and radiation therapy, together accounting for 90% of all treatments [4,5]. Prostate cancer yearly expenditures exceed $12 billion in treatment costs in the United States [6,7]. In addition to the high associated cost, current therapies are often time intensive and painful for the patient. Replacing current treatment methods with photothermal therapy could provide significant financial savings, cut down treatment time, and alleviate patient discomfort [8].

Plasmonic photothermal therapy (PPTT) is an efficient method of inducing localized hyperthermia using electromagnetic radiation. Use of PPTT for the purpose of cancer treatment has been widely studied as a minimally invasive and cost effective treatment modality [9]. For PPTT it is advantageous to utilize nanoparticles that transduce light to heat energy most efficiently at wavelengths of light that allow for the deepest penetration of blood and soft tissues. The near-infrared light region (800–1200 nm) offers good penetration, but gold and silver nanostructures such as nanospheres, nanocubes, and core–shell structures cannot reach surface plasmon resonance (SPR) peaks of these wavelengths, thus requiring a different approach. One such approach is to modify the geometric shape, and thus plasmon resonance of the nanoparticles. Gold nanorods (GNRs) for example, can be tuned to have SPR peaks from the visible range into the near-IR by increasing the length to width aspect ratio [10]. Another approach is to create hollow nanoparticles and vary the wall thickness and porosity to obtain the desired SPR peak, such as in gold nanocages (GNCs) [11].

Due to the challenging nature of creating hollow nanoparticles with controlled wall thickness and porosity, PPTT using such nanoparticle types has not been readily available until recently. Advancements made in the galvanic replacement reaction in which silver nanostructures serve as templates for hollow gold nanostructures with controllable size, wall thickness, and porosity has made way for the possibility of structures such as the gold nanocage to be utilized in cancer diagnostics and therapy [12].

* Corresponding author at: 36 S. Wasatch Dr., Salt Lake City, UT 84112-5001, USA.
E-mail address: hamid.ghandehari@pharm.utah.edu (H. Ghandehari).

http://dx.doi.org/10.1016/j.jconrel.2015.10.036
0168-3659/

The use of anticancer drugs within nano-based carriers offers a means of solubilizing and delivering hydrophobic drugs to the tumor site, as well as reducing distribution to other organs, and lowering the associated systemic toxicity [13,14]. The delivery of these drugs to solid tumors relies on the nanoscale size, which reduces the uptake into healthy tissues and takes advantage of the loose junctions between vascular endothelial cells in tumors, a phenomenon known as the enhanced permeability and retention (EPR) effect [15,16]. After permeation of the tumor, contact with receptors expressed on cancer cell surfaces can immobilize the nano-based carriers and trigger endocytosis and subsequent drug release [17]. Carriers in the 5–10 nm range are cleared rapidly from the body by urinary excretion, lessening the concerns of chronic toxicity and reducing uptake by healthy tissues. This also reduces tumor accumulation via EPR however, due to the reduced period of bioavailability [18]. With this in mind, there is a need to maximize polymeric delivery to the tumor within the bioavailability time period.

Current techniques for inducing hyperthermia, such as radiofrequency, ultrasound, or intraperitoneal perfusion are restrictive in their capacity and offer minimal selectivity toward cancerous tissues [19]. Hyperthermia induced by light absorption of plasmonic gold nanostructures allows for targeted, tissue specific localized heating. When light of a wavelength matching the SPR of the gold nanostructure interacts with the gold nanostructures, oscillations of the metallic electrons allow the light to be absorbed and for heat energy to be produced [20]. Nanostructures delivered to cancerous tissues via EPR can then be used to induce localized, tissue specific hyperthermia [21]. Our research group has previously shown that lasers can be used with gold nanoparticles to guide the delivery of macromolecules [18]. Elevated intratumoral temperatures produced by PPTT result in increased blood perfusion and vascular permeability, enhancing delivery of macromolecules by up to 1.8 fold [22]. The elevated temperatures also cause the expression of heat shock proteins that can be targeted, thereby increasing the delivery and retention of polymer therapeutics [18,22–25]. This technique allows for temperatures ranging from mild hyperthermia at 39 °C to 45 °C up to ablative hyperthermia at 50 °C to 70 °C. Combining a mild hyperthermic macromolecular drug delivery approach with a subsequent ablative hyperthermia delivered by the same nanoconstruct system could provide for a multi-pronged therapeutic approach allowing for simultaneous ablation of tumor tissue and blocking of the macromolecules from exiting the tumor site due to damaged tumor vasculature. While these findings have shown to enhance efficacy of prostate cancer therapy in mice, little is known about the fate of the gold nanoparticles. In addition comparative effects of gold nanorods and nanocages are unknown. In this work we aim to compare the biological and physicochemical properties of GNRs and GNCs in the context of prostate tumor delivery. Factors such as cytotoxicity, uptake, ablative potential, biodistribution, acute and chronic toxicity, and efficacy of macromolecular delivery in a prostate tumor model are explored.

2. Materials and methods

2.1. Preparation and characterization of nanoparticles

2.1.1. Gold nanorod synthesis

GNRs were synthesized using the seed-mediated growth method [26]. Optimization of silver nitrate content and the seed amount yielded GNRs with an aspect ratio of 4.05 such that the SPR peak was 812 nm. After centrifugation and washing with deionized water, methoxy-poly (ethylene glycol) (mPEG) (5 kDa, Creative PEGWorks, Chapel Hill, NC) was added to the GNR suspension and stirred for 1 h at a final PEG concentration of 100 μM. The mPEG GNR mixture was then dialyzed (3.5 K MWCO, Spectrum Labs, Rancho Dominguez, CA) for 3 days to remove cetyltrimethylammonium bromide (CTAB) and excess unbound mPEG. The colloid was then concentrated via centrifugation.

2.1.2. Gold nanocage synthesis

GNCs were synthesized with an SPR peak at 81 nm using a galvanic replacement reaction between silver and gold [12]. The literature methods were modified by running 1.2 L/min of argon across the top of the silver cube synthesis reaction to minimize oxidation effects, as well as increasing the volume size by 10 fold and running the reaction in a 250 mL round bottom flask. A 19 mm egg shaped Teflon coated magnetic stir bar was used for stirring at 350 rpms. Temperature was held at 149 °C throughout the reaction. For the galvanic exchange between gold and silver, 0.5 mL of as synthesized silver cubes was added to a 100 mL round bottom flask with 5 mL of 1 mg/mL poly(vinyl pyrrolidone) (PVP) (M_g = 55,000, Aldrich). The contents were then titrated via a syringe pump at a rate of 0.8 mL/min with 0.2 mM $HAuCl_4$ to approximately 16 mL. The titration was monitored by removing small aliquots with a glass Pasteur pipette and read spectrophotometrically to determine the SPR peak. The GNCs were then washed 3 times via centrifugation with deionized water and conjugated with 5 kDa mPEG, at an equivalent concentration compared to GNRs and stirred for 1 h. The mPEG GNC mixture was then centrifuged, washed, dialyzed, and concentrated in the same manner as the nanorods.

2.1.3. Gold nanorod and nanocage characterization

Characterization of the nanoparticles was performed by UV–Vis-NIR spectrophotometry (Fig. 1), dynamic light scattering (DLS), and transmission electron microscopy (TEM). One hundred individual particles for each system were measured from TEM micrographs in order to obtain approximate size distributions. Due to the effect mPEG has on hydrodynamic radius, the average particle size reported by DLS was approximately 10 nm larger than that measured by TEM. The addition of mPEG to the gold nanoparticles was also found to blueshift the absorbance peak by 5–10 nm depending on the particle type. For example, the bare GNRs yielded a peak absorbance at 812 nm, whereas the mPEG bound GNRs yielded a peak absorbance at 807 nm, and had dimensions of 60 × 14.8 ± 6.5 × 2.0 nm (Fig. 1). The nanorods measured zeta potential was −11.0 mV. This reaction was highly repeatable and accomplished in multi-liter batches. It was also possible to control the adsorption spectra and SPR peak by varying the silver nitrate content. The bare GNCs resulting from a galvanic exchange had a peak absorbance at 810 and the mPEG bound GNCs had a peak absorbance at 802 nm. The TEM measured particles had an edge length of 50 nm ± 7 nm (Fig. 1). It was possible to tune the absorbance peak by controlling a titration of 0.2 mM $HAuCl_4$ via a syringe pump at a rate of 0.8 mL/min. The measured zeta potential for the nanocages was −9.2 mV.

2.1.4. Comparison of ablative potential and ICP-MS

To compare light to heat conversion proficiency at the SPR peak, each colloidal suspension was diluted to an optical density of 2.00.

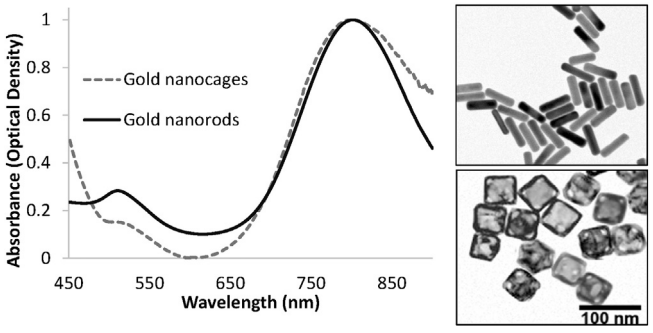

Fig. 1. Gold nanorod and gold nanocage absorbance spectrum. Optical densities at peak SPR were matched via dilution from stock solutions for easier comparison of overall absorbance spectrum. TEM of nanorods and nanocages. TEM image of GNRs (top) with length and width of 60 × 14.8 ± 6.5 × 2.0 nm. TEM image of GNCs (bottom) with edge length of 50 ± 7 nm, 100 nm. The scale bar applies to both TEMs.